

## Chapter 8

### **Fabrication of Mold with Thermosetting Polymer Patterns through Imprint Technology for Three Dimension Devices**

#### **Abstract**

Mold fabrication for imprinting can be significantly simplified by using specialized crosslinking polymers for pattern definition on silicon wafer. The thermosetting polymer pattern can be used on silicon molds for imprint technology because of two possibilities: (1) the silicon oxide molds with thermosetting polymer pattern can be obtained by any conventional semiconductor technology; (2) thermosetting polymers have no obvious  $T_g$  because of cross-linking structure, whereas decreases the hardness as the increase of temperature over their  $T_g$ . In this work, the Su-8 resist is used as the thermosetting polymer pattern on silicon wafer for molds. Thermal properties of the thermosetting and thermoplastic polymers were tested for imprinting pattern and imprinted resist. The hill-like structure fabricated by electron beam strategy for thick film was used to increase the adhesion between pattern and silicon wafer. The resolution of the thermoplastic polymer resist pattern imprinted by thermosetting polymer pattern was investigated by SEM. The shrinkage factor of the feature size after separation between thermosetting polymer pattern and thermoplastic polymer resist was used to define the feature size after imprinting. In addition, a microlens of polydimethyl siloxane (PDMS) has been fabricated by replication using the thermoplastic polymer resist after imprinting by the mold with microlens structure of the thermosetting polymer (SU-8).

## 8.1 INTRODUCTION

The application of nanofabrication to printing has a potential to develop into a competitive parallel process to serve the future technological demands of nanoelectronics and related areas. Nanoimprint lithography (NIL) is a very useful technique to fabricate various nanostructure devices such as a quantized magnetic disk.[1–4]. The resist pattern is fabricated by deforming the physical shape of the resist. The technique has excellent resolution with pattern less than 10 nm in a large area that can be realized with high throughput and low cost. A conventional mold is usually delineated by electron beam lithography and dry etching but it usually results in two-dimensional pattern.

Thermal imprint lithography is a promising method to fabricate integrated fine pattern using various materials.[5] In thermal imprint lithography, a thermoplastic polymer is heated above its glass transition temperature ( $T_g$ ), and a fine mold is pressed on the polymer. After cooling down below its  $T_g$ , the mold is released and the fine pattern on the mold is transferred to the polymer. Using thermal imprint processes, fabrication of high aspect ratio pattern,[6] curved cross-sectional pattern,[7] and fine pattern transfer on novel plastic plates,[8] have been reported.

A mold is pressed into a thin polymer layer heated above its glass transition temperature ( $T_g$ ), then cooled to a temperature below  $T_g$  of the polymer, and the mold is released. The residual resist layer in the compressed areas is finally removed from the substrate by oxygen plasma etching. Molds used in NIL are usually fabricated by a multi-step procedure. A double resist layer is spin-coated on wafer and patterned by e-beam lithography. Chromium deposition, lift-off and reactive ion etching of the Chromium mask are carried out to define the stamp pattern [9].

Crosslinking plastics, so-called thermosetting polymers, are increasingly used as engineering materials because of their excellent stability toward elevated temperature

and physical stress. They are dimensionally stable under a wide variety of conditions due to their rigid network structure. Such polymers will not flow when heated above their  $T_g$ , while thermoplastic polymers tend to soften and flow when heated. Therefore, the thermosetting polymer is able to be the mold for imprint. In this case, imprint has to be performed on thermoplastic polymer surface by thermosetting polymer pattern.

In this chapter, hill-like structures are fabrication by e-beam lithography to increase the stickiness between the thermosetting polymer pattern and the silicon wafer. Such a hill-like structure prevents the lift-off of the thermosetting polymer pattern from silicon wafer when it is separated from the thermoplastic polymer resist. In addition, we have demonstrated that the fabrication of working molds with thermosetting polymer pattern and their applications for NIL such as micro-lens fabricated by PDMS.



## **8.2 EXPERIMENT**

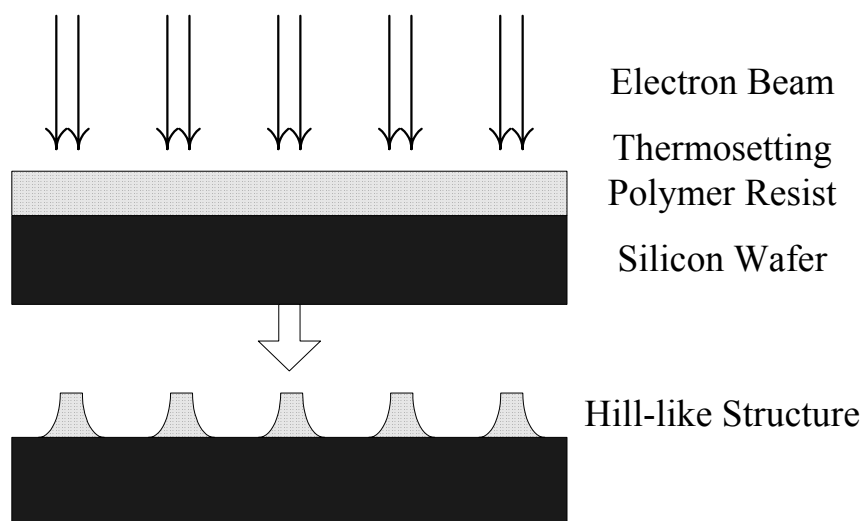
### ***8.2.1 Thermosetting Polymer Patterns***

The SU-8 resist from the Microchem Company (Massachusetts) was used to fabricate the thermosetting polymer pattern with the aid of an electron beam. The ingredients of the resist, provided from the vendor, are 50%–70% epoxy resin, 25%–50% g-butyrolactone, and 1%–5% propylene carbonate and triarylsulfonium hexafluoroantimonate salts. Electron-beam exposure was carried out using a Leica Weprint Model-200 stepper (Jena, Germany). The shaped electron-beam energy was 40 kV with a beam size of 20 nm and a beam current of 40 A/cm<sup>2</sup>. The developer for the SU-8 resist was a 98%–100% 1-methoxy-2-propyl acetate solution. The SU-8 resist was spun onto a 6 in. silicon wafer, with resist thickness of 3.5  $\mu\text{m}$  at a spin rate of 6000 rpm for 0.5 min, followed by a soft-baking process for 10 min at 65 °C and 2

min at 90 °C. The glass transition temperature was measured with a differential-scanning calorimeter (Seiko SSC-5000) and by the wafer-curvature measurement (Tencor FLX-2320), the stress variation of thin film coated on substrate during heating procedure of the imprint. The feature size was evaluated using a cross-sectional SEM (Hitachi S-4000).

### 8.2.2 Mold with Thermosetting Polymer Patterns Fabrication

The SU-8 resist, a thermosetting polymer resist, was exposed by electron beam with dosage of 15  $\mu\text{C}/\text{cm}^2$ , followed by developing and hard-baking processes for 10 min at 105 °C. In the case of a thick film exposure, the multi-layer structures can be fabricated through e-beam exposure resulting in hill-like structure due to the scattering effect as shown in Scheme 8-1. [10] The trichloro(1H, 1H, 2H, 2H-perfluorooctyl)silane (FOTS) was used as the precursor for self-assembled monolayers (SAM) on mold with the thermosetting polymer pattern as the mold



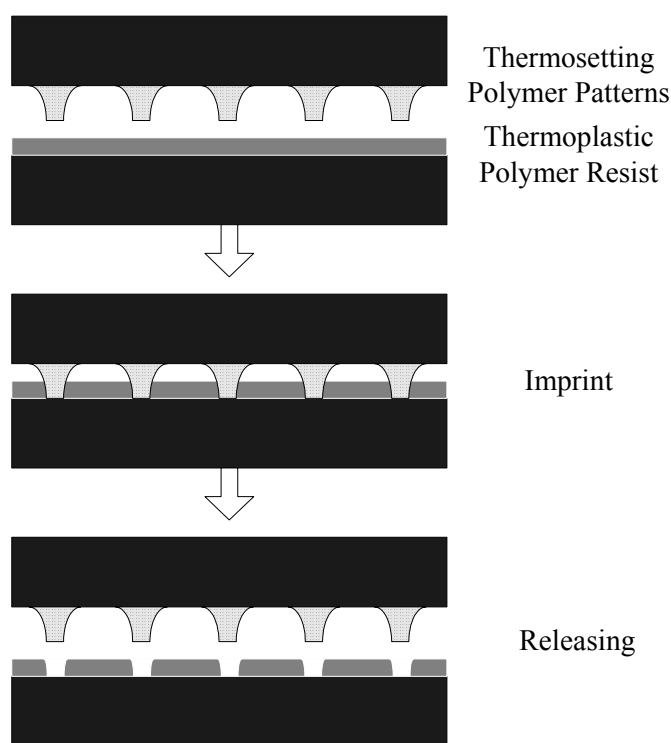
**Scheme 8-1.** The hill-like structure fabricated using electron beam strategy for thickness film.

releasing and anti-sticking layer for imprint that was purchased from Aldrich and used

as received.

### 8.2.3 Imprint Process

The resist (22A4), purchased from Sumitomo Chemical Company of Japan was used for imprint. The success of the combination of resist and mold surface modifications can be demonstrated using an imprint tool developed by Nanonex (nx-1000, US). For multiple imprint investigations, an experimental series of 50 imprints are continuously printed with one mold on two silicon wafers. These two



**Scheme 8-2.** The imprint process by using mold with hill-like structure of the thermosetting polymer.

wafers are printed with 25 imprints each, with a spacing of 1 mm in between. The mold with thermosetting polymer pattern has a size of 1 X 1 cm<sup>2</sup> containing test structures with a depth of 2 μm. These feature structures consist of lines and dots. The contact between resist and mold had preprint pressure of 200 psi at preprint

temperature of 110 °C, and then an imprint force of 380 psi was used to press the mold into a 700-nm thick resist with duration of 5 min at 130 °C. The imprint processes are shown in Scheme 8-2.

### 8.2.4 Surface Energy Calculations

Surface energy is directly related to the stickiness between the thermosetting polymer pattern and thermoplastic polymer resist, which is evaluated using the Lifshitz-van der Waals acid-base approach (three liquid acid-base method) previously proposed by van Oss et al. [11,12] This methodology introduces a new concept of “apolar” (Lifshitz-van der Waals,  $\gamma^{LW}$ ) and “polar” (Lewis acid-base,  $\gamma^{AB}$ ); the latter cannot be represented by a single parameter such as  $\gamma^p$ . Briefly, the theoretical approach follows the additive concept suggested by Fowkes.[13]

$$\gamma = \gamma^d + \gamma^{AB} \quad (1)$$

where  $\gamma^d$  stands for the dispersive term of the surface tension. The superscript AB refers to acid-base interaction. By regrouping the various components in eq (1), the surface energy can be expressed as:

$$\gamma = \gamma^{LW} + \gamma^{AB} \quad (2)$$

In addition, two parameters are created to describe the strength of the Lewis acid and base interactions:

$\gamma_s^+$  = Lewis acid parameter of surface free energy

$\gamma_s^-$  = Lewis base parameter of surface free energy

$$\gamma^{AB} = 2(\gamma_s^+ \gamma_s^-)^{1/2} \quad (3)$$

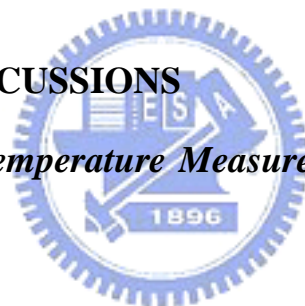
van Oss, Good, and their co-workers [11,12] developed a “three-liquid procedure” (eq 4) to determine  $\gamma_s$  by the contact angle technique.

$$\gamma_L (1 + \cos \theta) = 2 \left[ (\gamma_s^{LW} \gamma_L^{LW})^{1/2} + (\gamma_s^+ \gamma_L^-)^{1/2} + (\gamma_s^- \gamma_L^+)^{1/2} \right] \quad (4)$$

To determine the components of  $\gamma_S$  of a polymer solid, three liquids are needed, two of them are polar and the third one is apolar. The polar pairs, water and ethylene glycol, or water and formamide, are recommended to give good results. The apolar liquid is either diiodomethane or R-bromonaphthalene because the Lewis acid and Lewis base parameters of these liquids are readily available. The LW, Lewis acid, and Lewis base parameters of  $\gamma_S$  can then be determined by solving these three equations simultaneously. By measuring contact angles for these three well-characterized (in terms of  $\gamma_L^{LW}$ ,  $\gamma_L^+$  and  $\gamma_L^-$ )[14,15] liquids, three equations with three unknowns are generated. Water, diiodomethane, and ethylene glycol were the three liquids employed in this study.

## 8.3 RESULTS AND DISCUSSIONS

### 8.3.1 *Glass Transition Temperature Measurement and Surface Energy Analysis*



The imprint technique is based on the diversity of glass transition temperatures ( $T_g$ ) between the thermosetting polymer pattern and the thermoplastic polymer resist. Therefore, it is important to measure the phase-transition temperature of the resist material. In this study, the conventional DSC method was used to determine glass-transition temperatures of the thermosetting polymer pattern and thermoplastic polymer resist for imprint application. Figure 8-1 shows the DSC curves of the thermosetting polymer (SU-8) and thermoplastic resist (22A4) where the endothermic peak at around 50 °C is probably due to the endothermic effect of the resist additive. The endothermic peak at around 102 °C is caused by the glass transition of the thermoplastic polymer resist. The glass transition temperature of thermosetting polymer is not clearly defined from the DSC curve due to the nature of the cross-link

structure. The glass transition temperature of the thermosetting polymer is closed to 272 °C, significantly higher than the  $T_g$  of thermoplastic polymer resist. Therefore, the the thermosetting polymer pattern maintains as a high modulus solid at 150 °C of the imprint temperature.

Another method for measuring phase-transition temperatures is by the wafer-curvature measurement (WCM) which is usually performed with a stress measurement instrument to measure the radius of curvature and stress variation of thin films coated on the substrates during a pre-determined the heating procedure.[16] In our experiment, thermosetting polymer resist and thermoplastic polymer resist coated on a silicon substrate were used for stress measurement. The heating rate was held at 10 °C/min and the ambient gas was air. As shown in Figure 8-2, the stress for thermoplastic polymer resist varies from 30 MPa to -30 Mpa. Figure 8-2 indicates that the phase-transition temperature of thermoplastic polymer resist is about 105 °C. The value of  $T_g$  measured by this WCM method is only slightly different from that obtained from DSC for thermoplastic polymer resist. The glass transition temperature for thermosetting polymer can not be detected by this WCM method due to the cross-link structure mentioned above. This thermosetting polymer shows stable stress as the temperature is increased above 100 °C. The DSC technique measures the calorimetric transition, while in contrast, the WCM technique detects the mechanical relaxation transition.

### ***8.3.2 Contact Angle and Surface Free Energies***

Stickiness is present during the separation process of NIL. Strong adhesion can come from the capillary, electrostatic force, van der Waals force, or in some cases by the hydrogen bonding. In a imprinting, the transfer of pattern from the mold to the



resist on the substrate requires complete antiwetting surface of the mold to minimize defects induced by stickiness. The value of surface energy is commonly used as an indicator for the stickiness characteristics of materials. [17, 18] The values of  $\gamma_L^{LW}$ ,  $\gamma_L^+$  and  $\gamma_L^-$  were calculated by contact angles of water, diiodomethane, and ethylene as shown in Table 8-1. Contact angles for these three liquids are used to calculate the respective surface energies. Plots of critical surface energy as a function of temperature are displayed in Figure 8-3. In general, the surface energy of a polymer decreases only slightly with the increase of temperature.[16,17] The surface energy of the thermoplastic polymer resist decreases with the increase of temperature and the surface energy is about 43.5 mJ/m<sup>2</sup> at 150 °C for imprint temperature. This result indicates that the thermosetting polymer is suitable for imprinting application.

### ***8.3.3 Mold with Thermosetting Polymer Patterns and the Imprinted Patterns***

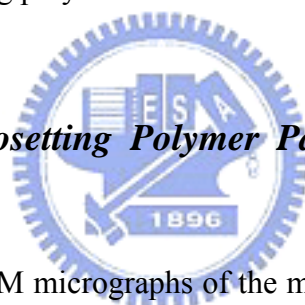


Figure 8-4 shows the SEM micrographs of the mold with thermosetting polymer pattern. The thermosetting polymer pattern of dense lines possesses hill-like structure for fabricating the trench pattern by the imprint process as shown in Figure 8-4 (a). The formation of such hill-like structure of the thermosetting polymer is caused by the scattering effect of the electron beam.[18] The hill-like structure of the thermosetting polymer increases the contact area between the pattern and the silicon wafer surface, resulting in the increase of stickiness for avoiding lift-off during separation step in imprint process. The feature size on the top of hill-like structure of these dense lines is about 835 nm. Figure 8-4 (b) shows the hill-like structure of the thermosetting polymer of dense cylinders for fabricating the contact holes by the imprint process. The height of the hill-like pattern for iso-lines and cylinders is about 3.5  $\mu\text{m}$ .

Figures 8-4 (c) and 4 (d) show SEM micrographs of the thermoplastic polymer resist with 650 nm thickness after separation from the mold of the thermosetting polymer pattern of hill-like iso-lines and dense cylinders under a typical process temperature of about 150°C and a typical pressure of about 100 bar. The thermosetting polymer pattern for negative tone transfers the feature to the thermoplastic polymer resist for positive tone, resulting in the pattern of iso-trenches and dense contact holes. The feature size of the iso-trenches and dense contact holes on the thermoplastic polymer resist surface is smaller than that of the iso-lines and dense cylinders on the mold of the thermosetting polymer pattern. In a hot embossing lithography, the feature size of the thermoplastic polymer resist shrinks slightly after cooling down below its  $T_g$ , while feature size of pattern on the mold is closed to a constant since the thermal extension for coefficient of the silicon wafer mold is significantly lower than that for resist. In this work, both thermosetting polymer and thermoplastic polymer shrink after cooling down, resulting in tight contact between the thermosetting and thermoplastic polymers. The adhesion between the thermosetting and the thermoplastic polymer drives the thermoplastic polymer to shrink the feature size as the thermosetting polymer pattern separates from the thermoplastic polymer. A useful relative measure of the shrinkage factor was calculated from the relationship  $f = 1 - (d_t/d_l)$ , where  $d_t$  is the feature size of iso-trench on thermoplastic polymer surface and  $d_l$  is the feature size of iso-line for thermosetting polymers. The shrinkage factor ( $f$ ) increases with the increase of the feature size of the iso-line of the thermosetting polymer as shown in Figure 8-5. This observation suggests that the adhesion between thermosetting and thermoplastic polymers increases with the increase of contact area, the larger feature size pattern possesses larger contact area and results in larger value of shrinkage factor. The total contact area between thermosetting and thermoplastic polymers for imprinting trench

is larger than that of the imprinting single hole, resulting in larger value of shrinkage factor from the trench imprint.

#### **8.3.4 Fabrication of Microlens**

Three-dimensional (3D) structures are required in various devices such as optical devices (microlenses, photonic crystals, etc.). Electron beam lithography is very useful for the fabrication of 3D structures, as we demonstrated previously with the hill-like structure. [10] Figure 8-6 (a) shows scanning electron micrograph (SEM) image of the micro-lenses of the thermosetting polymer fabricated by exposure strategy through electron beam on a silicon wafer. Figures 6 (b), (c), and (d) show various thermosetting polymer microlens fabricated by dividing the circle pattern into five section with the same the center of a circle, then electron beam exposed the five sections of 10, 8, 6, 4, and 2  $\mu\text{C}/\text{cm}^2$  dosages respectively as shown in Figure (6). The unit distances of the micro-lens as shown in Figures 6 (b), (c), and (d) are 3, 5, and 7  $\mu\text{m}$ , resulting in the radii of 12.5, 17.6, and 33.8  $\mu\text{m}$  of these lens, respectively. The curvature radius of the microlens increases with the increase of the unit distance. Figures 8-7 (a), (b) and (c) show SEM images of the thermoplastic polymer resist imprinted microlens patterns with various curvature radii as given in Figures 8-6 (b), (c), and (d), respectively.

Polydimethyl siloxane (PDMS) was used in a soft lithography technique as a replication material.[22,23] The soft lithography is a nonphotolithographic fabrication process based on self-assembly and replicated molding. It provides a convenient, effective, and low-cost method for the formation and manufacturing of micro- and nanostructures with feature sizes ranging from 50 nm to 100 mm. In this work, the thermoplastic polymer resist containing a reverse microlens pattern, as shown in

Figure 8-7 (a), was obtained by imprinting onto the PDMS that was coated on a silicon wafer by using a NIL apparatus. The PMMA surface was precoated by a thin layer of silane-coupling agent to reduce the critical surface tension.

Scheme 8-3 shows the schematic of the fabrication process of the PDMS microlens using the NIL apparatus. The reverse microlens mold of the thermoplastic polymer resist was prepared by the imprinting process as mentioned in section 3.3. The PDMS was then cast onto the reverse microlens mold which was pressed onto a silicon bare wafer using the NIL apparatus. The PDMS film thickness was controlled by the imprinting pressure. The PDMS was baked at 75 °C for 15 min during pressing. After pressing, PDMS was stuck on an upper silicon bare wafer and was removed from the thermoplastic polymer resist reverse microlens mold. In this way, the PDMS microlens was fabricated. Figures 8-8 (a) and (b) shows the top view and side-view 3D SEM images of the PDMS microlens, respectively. The resulted radius and height were 10.2, and 3.2  $\mu\text{m}$ , which are nearly the same as those of the reverse microlens mold of thermoplastic polymer resist on silicon wafer.

## 8.4 CONCLUSIONS

The mold pattern using thermosetting polymer has been fabricated in imprint process, simplifying the etching and resist removing processes for mold fabrication. The hill-like structure fabricated by electron beam for thick film is able to prevent the thermosetting polymer pattern lift-off from the silicon wafer surface when it is separated from thermoplastic polymer resist. Two and three dimensional patterns were fabrication by using the thermoplastic polymer resist with dimensions of 650 nm and 3.3  $\mu\text{m}$  for imprinting by the mold with the thermosetting polymer pattern. The shrink effect was found as the thermosetting polymer pattern separating from thermoplastic

polymer resist under 2D imprint process. Three-dimensional microlens mold fabrication has been demonstrated by exposure strategy through electron beam. Various 3D microlens molds were delineated by increasing of the unit distance for electron beam exposure. Then, the mold was imprinted onto the thick thermoplastic polymer resist by a NIL apparatus. As a result, it was confirmed that a 3D mold, after the NIL, kept its original shape, and 3D structures were successfully imprinted onto the thermoplastic polymer resist. These results revealed that the 3D mold fabricated by electron beam lithography can be applied to the NIL. Furthermore, a PDMS microlens has been fabricated by using a thermoplastic polymer resist reversal microlens mold. This study has demonstrated that the mold with thermosetting polymer pattern is very useful to fabricate 2D pattern or 3D optical device such as a microlens.



## REFERENCES

1. S Y. Chou; P. R. Krauss; P. J. Renstrom. *Appl. Phys. Lett.* **67**, 3114 (1996)
2. S Y. Chou; P. R. Krauss; P. J. Renstrom. *Science*, **272**, 85 (1996).
3. S Y. Chou; P. R. Krauss; W. Zhang; L. Guo; L. Zhuang. *J. Vac. Sci. Technol. B* **15**, 2897 (1997)
4. S. Okazaki. *J. Vac. Sci. Technol. B*, **9**, 2829 (1991).
5. S. Y. Chou; P. R. Krauss; P. J. Renstrom. *Appl. Phys. Lett.* **67**, 3114 (1995).
6. Y. Hirai; T. Yoshikawa; N. Takagi; S. Yoshida; K. Yamamoto. *J. Photopolym. Sci. Technol.* **16**, 615 (2003).
7. Y. Hirai; S. Harada; H. Kikuta; Y. Tanaka; M. Okano; S. Isaka; M. Kobayasi. *J. Vac. Sci. Technol. B*, **20**, 2867 (2003).
8. Y. Hirai; N. Takagi; S. Harada; Y. Tanaka. *Sens. Micromach. Soc.* **122**, 404 (2002).
9. L. Montelius; B. Heidari; M. Graczyk; T. Ling; I. Maximov; E. L. Sarve. *Proc. SPIE* **3997**, 442 (2000).
10. J. K. Chen; F. H. Ko, H. K. Chen; C. T. Chou. *J. Vac. Sci. Technol., B*, **22(2)**, 492 (2004).
11. C. J. van Oss; M. K. Chaudhury; R. J. Good. *Chem. Rev.*, **88**, 927 (1988).
12. C. J. van Oss; L. Ju; M. K. Chaudhury; R. J. Good. *J. Colloid Interface Sci.*, **128**, 313 (1989).
13. F. M. Fowkes. *J. Phys. Chem.* **66**, 382 (1962).
14. G. W. C. Kaye; T. H. Laby. Eds. *Table of Physical and Chemical Constants*, 15th ed.; Longman Scientific and Technical: Harlow (1992).
15. D. R. Lide; Ed. *Handbook of Chemistry and Physics*, 76th ed.; CRC Press (1995).
16. A. Schitz; P. J. Paniez. *Microelectron. Eng.* **27**, 413 (1995).

17. D. W. van Krevelen, *Properties of Polymers*, Elsevier, Amsterdam (1996)
18. M. Colburn; S. Johnson; M. Stewart; S. Damle; T. Bailey; B. Choi; M. Wedlake.  
*Proc. SPIE*, **3676**, 379 (1999)
19. S. Wu, *J. Macromol. Sci.*, **C10**,1 (1974).
20. B. B. Sauer; G. T. Dee. *Macromolecules*, **35**, 7024 (2002)
21. J. K. Chen; F. H. Ko, H. L. Chen; F. C. Chang, *Jpn. J. Appl. Phys.*, **42**, 3838 (2003)
22. Y. Xia; G. M. Whitesides. *J. Mater. Chem.* **7**, 1069 (1997)
23. Y. Xia; G. M. Whitesides. *Annu. Rev. Mater. Sci.* **28**, 153 (1998)

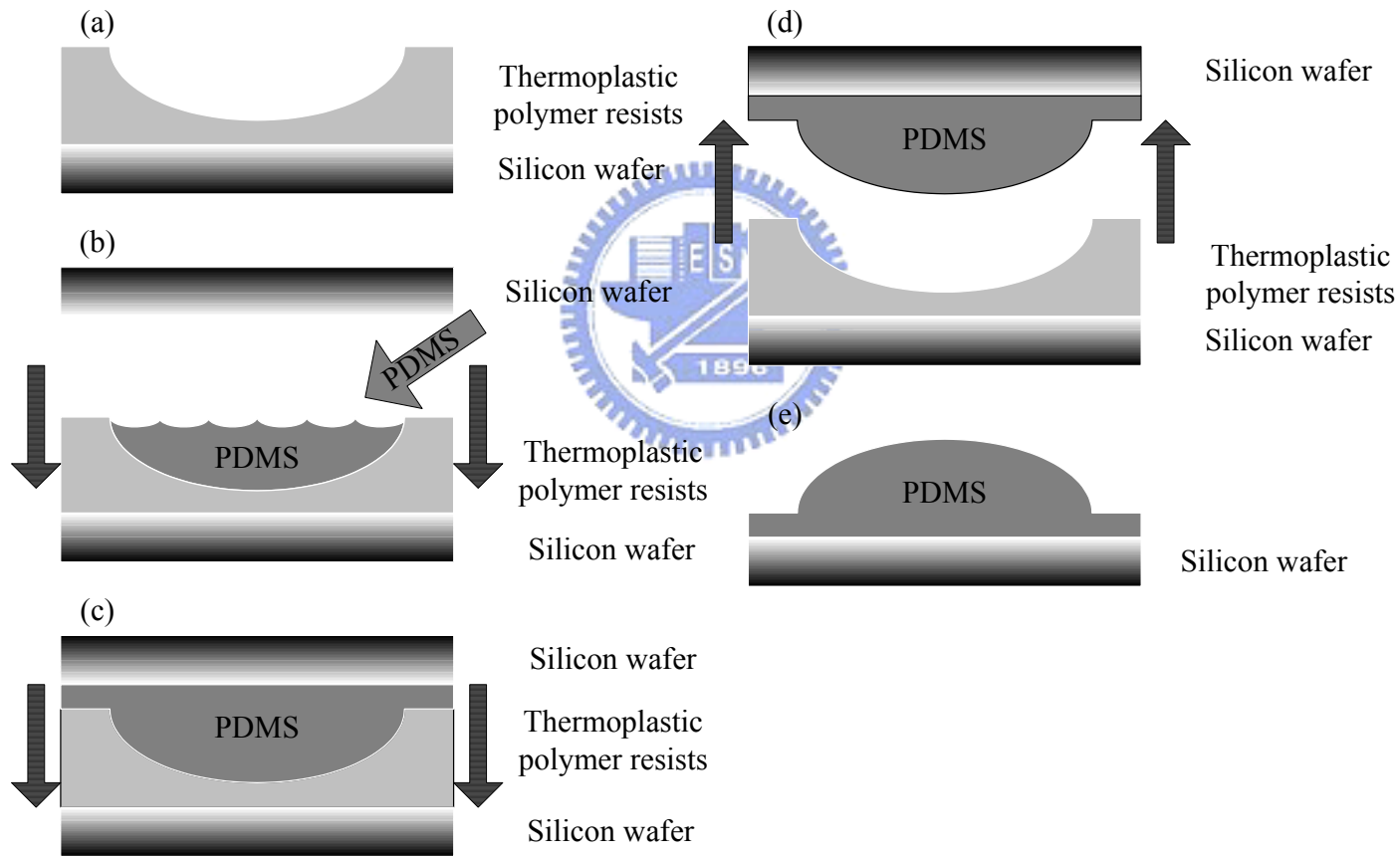


**Table 8-1.** Surface tension parameters calculated from the advancing contact angle for Water, Diiodomethane (*DIM*) and Ethylene Glycol (*EG*) on thermosetting polymer (SU-8) and thermoplastic polymer resists with the function of temperature.

Temperature (°C)	Contact angles for testing liquid (degrees)				Surface energy(mN/m)			
	Category	DIM	water	EG	$\gamma_{SLW}$	$\gamma_{S-}$	$\gamma_{S+}$	$\gamma_S$
25	22A4	59.1	81.1	49.1	40.21	4.80	2.04	46.47
	SU-8	38.8	71.6	51.0	29.09	0.46	7.08	32.68
45	22A4	59.3	81.4	49.7	39.56	4.63	2.09	45.78
	SU-8	40.1	72.2	51.6	28.98	0.45	6.95	32.52
65	22A4	59.7	81.5	50.2	39.36	4.43	2.06	45.40
	SU-8	40.5	72.8	52.2	28.75	0.49	6.86	32.40
85	22A4	60.0	81.6	51.1	38.95	4.35	2.06	44.94
	SU-8	41.3	73.2	52.7	28.58	0.57	6.58	32.44
105	22A4	60.2	82.0	51.2	38.69	4.00	2.05	44.42
	SU-8	41.8	74.1	53.4	28.46	0.48	6.67	32.06
125	22A4	60.6	82.1	51.4	38.28	3.86	2.07	43.93
	SU-8	42.6	74.6	53.9	28.23	0.49	6.69	31.85
145	22A4	60.7	82.3	51.8	38.17	3.80	1.99	43.68
	SU-8	42.8	75.0	54.5	28.17	0.49	6.60	31.76
165	22A4	61.0	82.8	51.9	37.86	3.76	1.96	43.28
	SU-8	43.4	75.4	55.1	28.00	0.39	6.73	31.24
185	22A4	61.3	83.0	52.2	37.60	3.74	1.89	42.91
	SU-8	43.9	75.8	55.8	27.83	0.38	6.71	31.03



**Scheme 8-3.** PDMS microlens fabrication. (a) Thermoplastic polymer resists imprinted by the mold with thermosetting microlens. (b) PDMS cast on thermoplastic polymer resists imprinted by the mold with thermosetting microlens.. (c) Press and bake PDMS using a NIL apparatus. (d) Remove Si wafer from PMMA. (e) PDMS microlens.



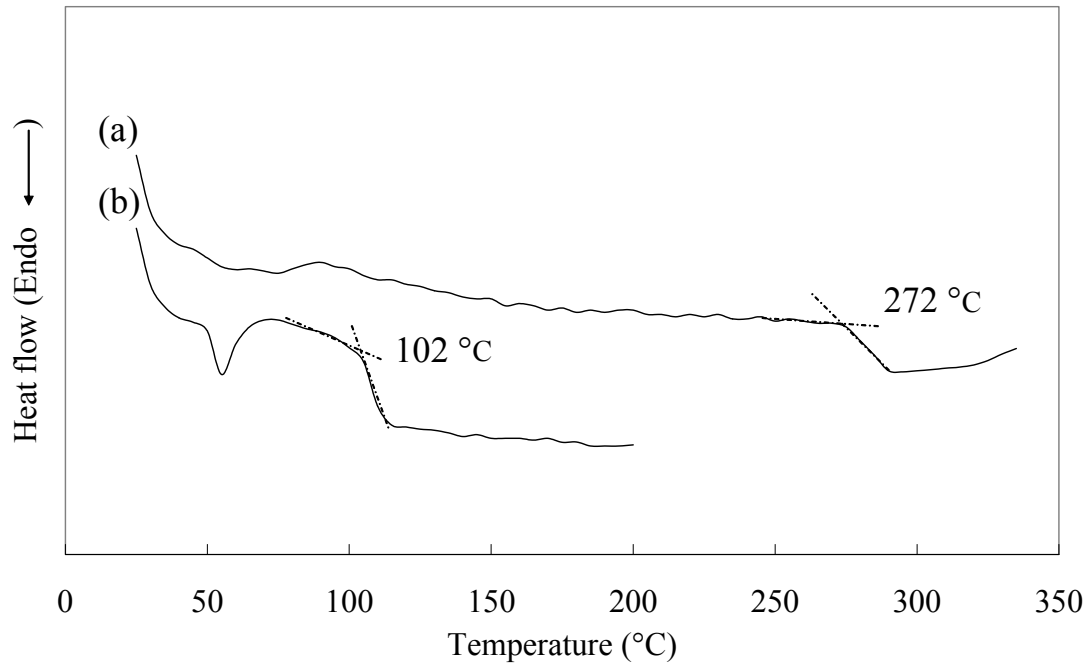


**Figure 8-1.** DSC curves of the chemical-amplified resist. (a) Thermosetting polymer (SU-8), and (b) thermoplastic polymer resists (22A4).

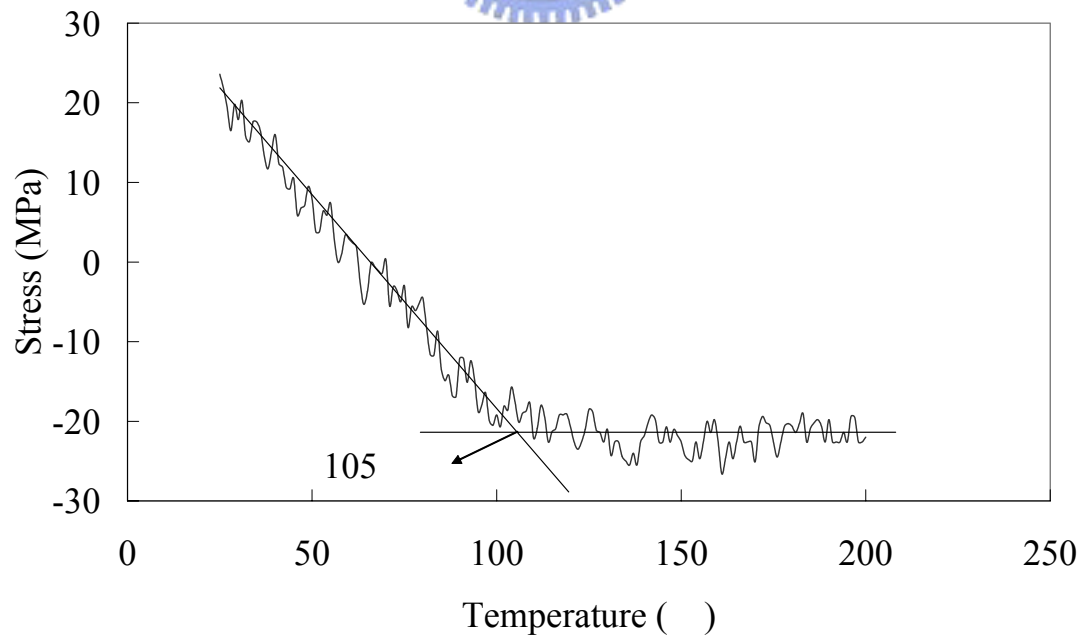


**Figure 8-2.** Plot of stress versus temperature for thermoplastic polymer resist (22A4).

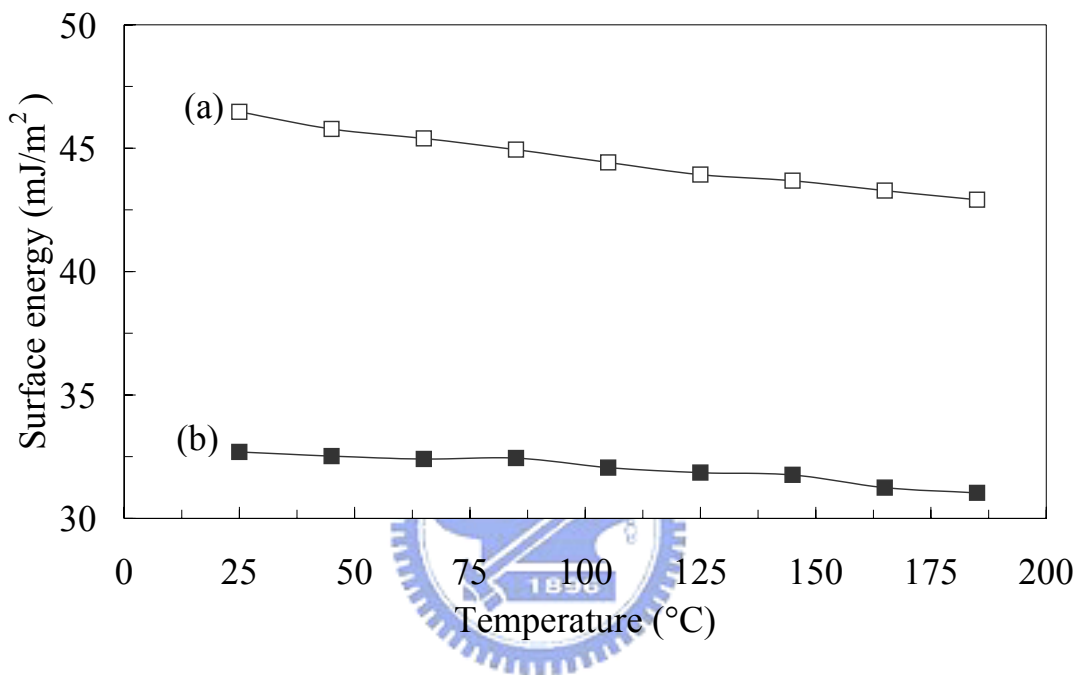


**Figure 8-3.** Surface energy versus temperature of (a) thermoplastic polymer resist (22A4), and (b) thermosetting polymer (SU-8). Surface energies were calculated from the contact angles of di-iodomethane, glycol and water as a function of anneal temperature.

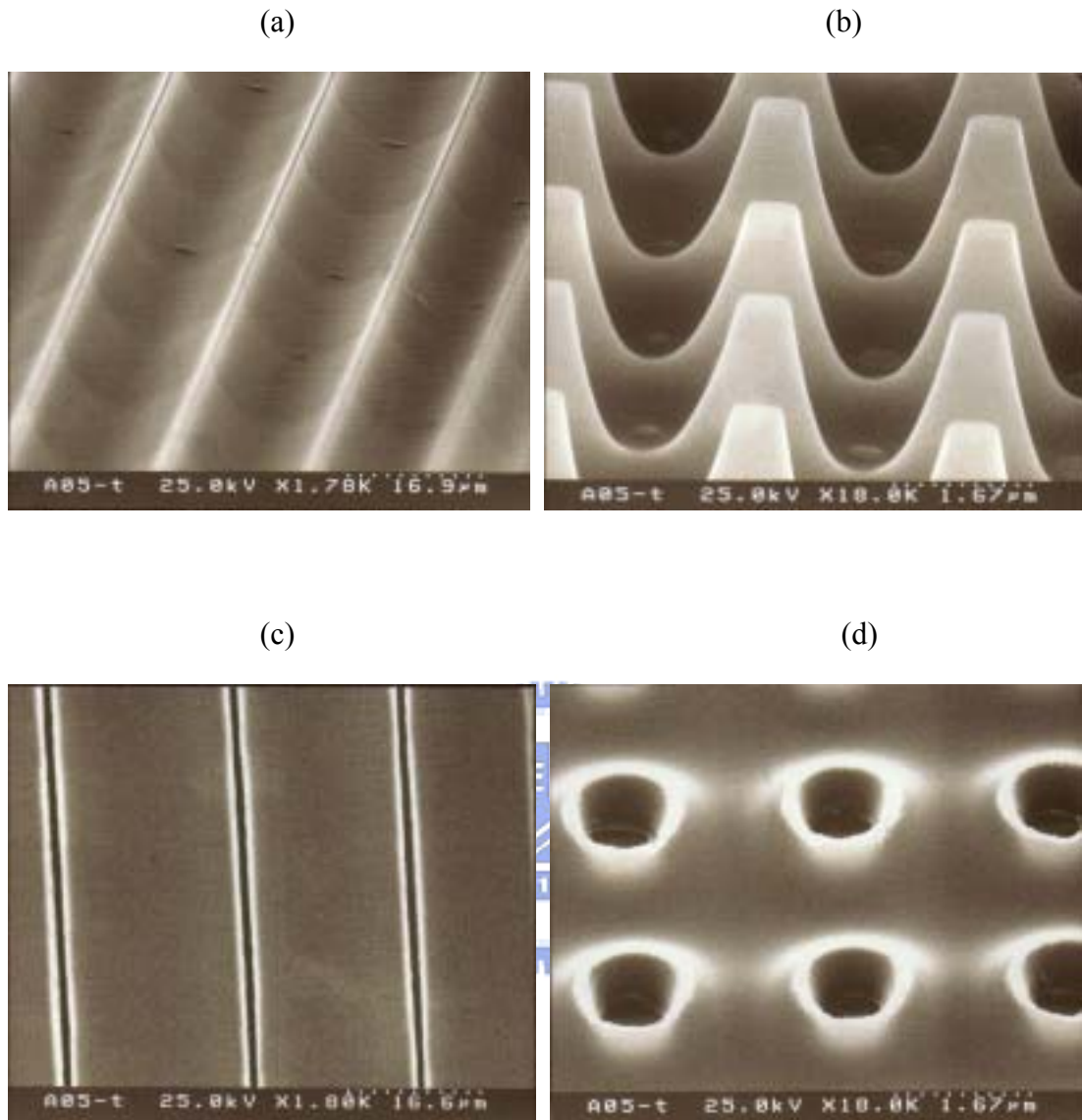


**Figure 8-4.** The SEM top-view images of the surface mold with thermosetting pattern (SU-8) for (a) iso-lines, and (b) dense cylinders. The thermoplastic polymer resist (22A4) with 650 nm of thickness imprinted by mold with thermosetting pattern (SU-8) for (c) iso-trenches and (d) dense contact holes.

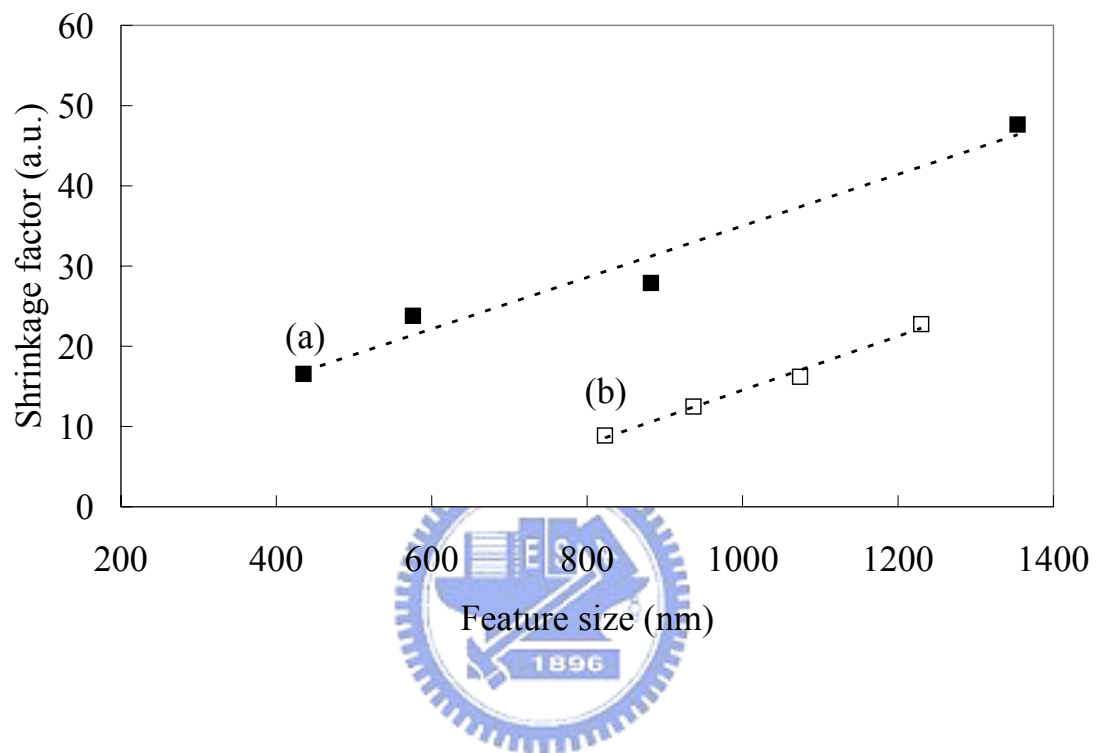


**Figure 8-5.** The shrinkage factor as a function of the feature size of thermosetting polymer pattern on mold for (a) iso-trenches, and (b) dense contact holes.

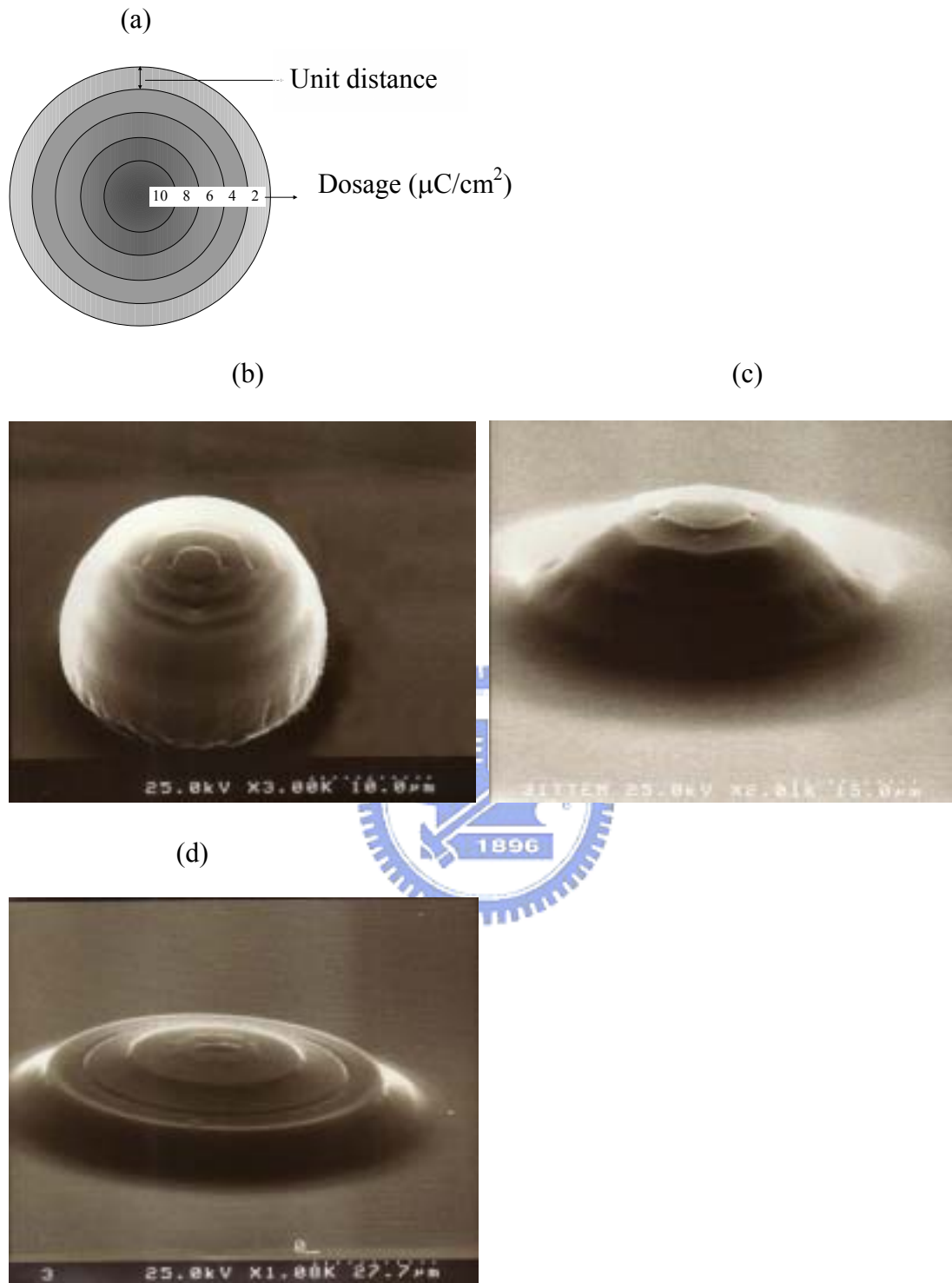


**Figure 8-6.** (a) The exposure strategy of electron beam for fabricating microlens of the thermosetting polymer. (b) The SEM images of 45°-tilt angle of the thermosetting polymer microlens for the mold before imprint as the unit distances are (b) 3  $\mu\text{m}$ , (c) 5  $\mu\text{m}$ , and (d) 7  $\mu\text{m}$ .

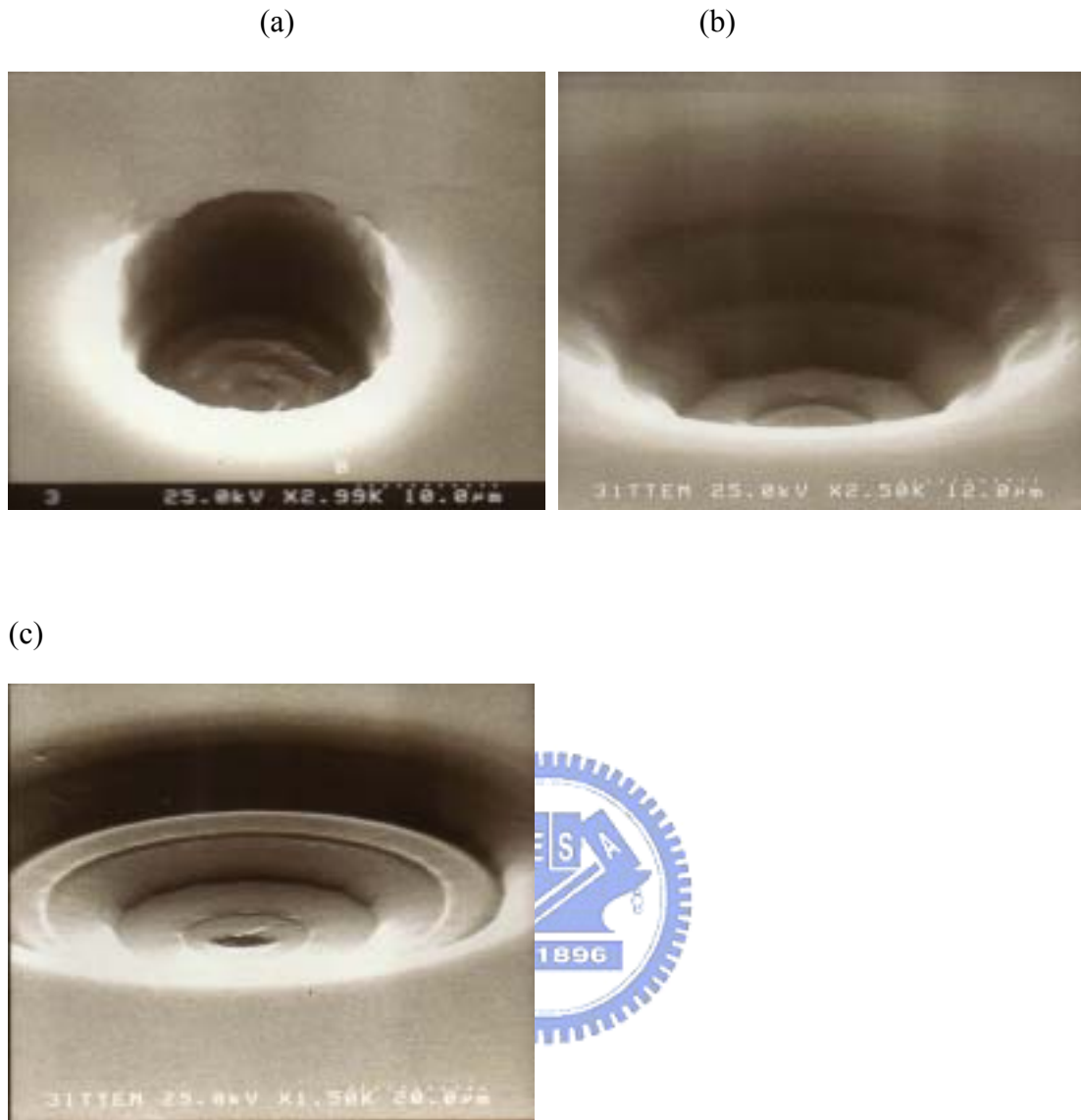
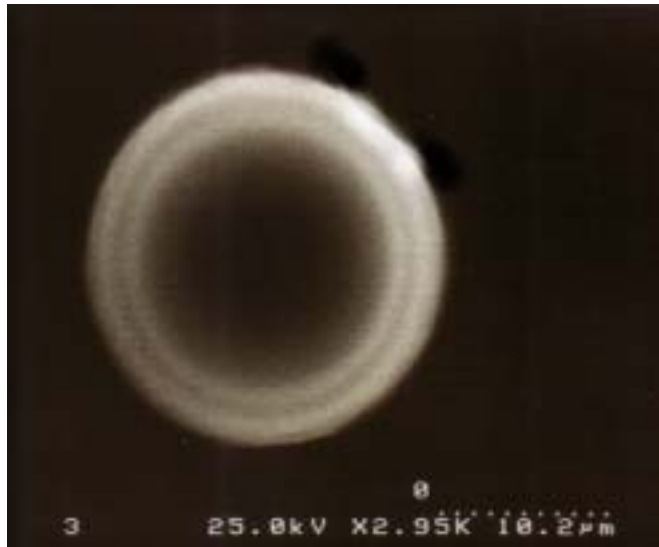


**Figure 8-7.** The thermoplastic polymer resist (22A4) with 3.3 μm of thickness imprinted by thermosetting microlenses molds. SEM images of 40°-tilt angle as thermoplastic polymer resist imprint the thermosetting microlens with (a) 3 μm, (c) 5 μm, and (d) 7 μm of unit distance.

(a)



(b)

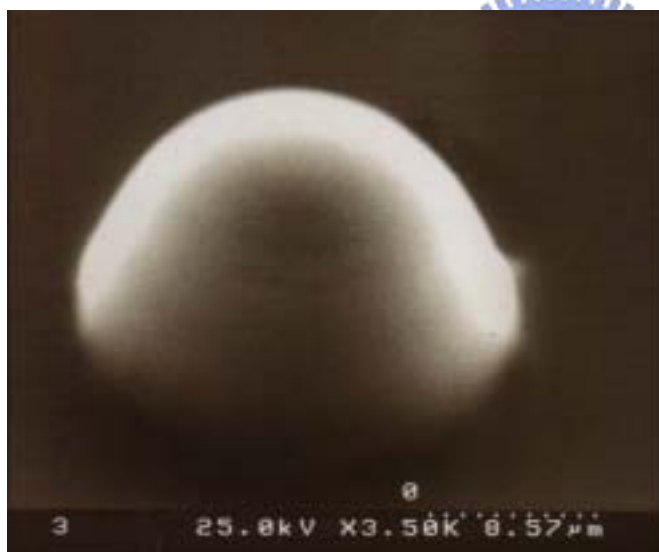


**Figure 8-8.** (a) SEM top-view image, and (b) SEM image of 40°-tilt angle for PDMS microlens fabricated by the reversal mold of thermoplastic polymer resist as unit distance is 3  $\mu\text{m}$ .